Hindawi Publishing Corporation
ISRN Spectroscopy
Volume 2013, Article ID 640896, 13 pages
http://dx.doi.org/10.1155/2013/640896

Research Article

C–H···F Hydrogen Bond and Integral Intensities of Vinyl C–H Vibtations in Push-Pull -Dimethylaminotrifluoromethyl Ketone and Its Deuterated Analog

Sergei Vdovenko, Igor Gerus, Elena Fedorenko, and Valery Kukhar

Institute of Bioorganic Chemistry and Petrochemistry, National Academy of Sciences of Ukraine, ul. Murmanska 1, Kiev 02094, Ukraine

Correspondence should be addressed to Sergei Vdovenko; sergiusz@bpci.kiev.ua

Received 22 August 2012; Accepted 26 September 2012

Academic Editors: M. Ma□czka and S. Pandey

The accurate analysis of infrared spectra (both wavenumbers and intensities) of (E)-4-(dimethylamino)-1,1,1-trifluorobut-3-en-2-one (DMTBN) and (E)-4-(hexadeutero-dimethylamino)-1,1,1-trifluorobut-3-en-2-one (d_6-DMTBN) revealed that besides intramolecular hydrogen bond C–H_β ··· F–C in the (EE) conformer, these enaminoketones form cyclic dimers between the (EZ) and (EE) conformers due to intermolecular hydrogen bonds, namely, C–H_α ···O=C and C–H_α ··· F–C. Evaluation of constant $K_{\text{H-complex}}$ and enthalpy of formation of these H-bonds ($-\Delta H$) revealed that C–H_α ···O=C bond has greater $K_{\text{H-complex}}$ and more negative ΔH than C–H_α ··· F–C bond (cf. 214.4 M^{-1}, −21.7 kJ $M^{-1}dm^3$, and 16.4 M^{-1}, −6.7 kJ $M^{-1}dm^3$, resp.). Consequently, stronger H-bond C–H_α ···O=C is formed in the first place, whereas weaker H-bond C–H_α ··· F–C is formed afterward. Moreover, formation of intermolecular C–H_α ··· F–C hydrogen bond has influence on C–F vibrations, but analysis of this influence must take into account the fact that these vibrations in some cases are coupled with δ_{CH_α}. True enthalpy of the equilibrium (EZ)⇌(EE) is positive (25.3 kJ $M^{-1}dm^3$), thus confirming results of DFT calculations, according to which the (EZ) conformer is more stable than the (EE) one.

1. Introduction

From spectroscopic experiments Allerhand and Schleyer [1] qualitatively concluded that the ability of a C–H group to form weak hydrogen bonds depends on carbon hybridization, as C(sp^1)–H > C(sp^2)–H > C(sp^3)–H and increases with the number of adjacent electron-withdrawing groups. The enhancement of the C–H donor strength by neighboring electronegative groups is often called "activation" of C–H. It is well known that hydrogen bonds in general are composed of different types of interactions [2]. As for all intermolecular interactions, there is a nondirectional "van-der-Waals" contribution, which is weakly bonding at long distances (by dispersion forces) and strongly nonbonding at short distances (by exchange repulsion). At their optimal geometry, van der Waals interactions contribute about 1 kJ mol^{-1} to the hydrogen bond energy. An electrostatic component (dipole-dipole, dipole-charge, etc.) is directional and bonding at all distances. It reduces with increasing distance and with reducing dipole moments or charge involved. For donors like O–H or N–H, the electrostatic component is the dominant one in hydrogen bond (several kJ mol^{-1}). This is also true for strongly polarized C–H groups (up to 8 kJ mol^{-1}), whereas for weakly polarized C–H groups the electrostatic component is of similar magnitude to the van der Waals contribution [3]. Only for the strongest types of hydrogen bonds does a charge-transfer component become important [2]; it does not play a relevant role for weak C–H···F interactions. The above circumstances have far-reaching consequences. Firstly, electrostatic component varies smoothly with varying geometry and diminishes only slowly with increasing distance; this leads to a pronounced softness of the hydrogen bond geometry. The C–H···F interactions can be easily stretched, compressed, and bent from optimal geometry. Secondly,

the bonding situation is strongly dependent on the donor and acceptor polarizations; therefore, weak hydrogen bonds involving polarizable groups can be critically influenced by their surroundings. Thirdly, with falling C–H polarization, the directional electrostatic component is reduced, whereas the isotropic van der Waals component is unaffected; the net interaction therefore loses directionality. Fourthly, upon compression, the van der Waals contribution becomes repulsive and might even result in a positive (i.e., nonbonding) net energy; this will be more important than the smaller the electrostatic component is. In C–H⋯F bonds, the net charge on carbon may be negative; this is the classical hydrogen bonding situation ($C^{\delta-}$–$H^{\delta+}$ ⋯$F^{\delta-}$). Carbon may also carry a positive partial charge ($C^{\delta+}$–$H^{\delta+}$ ⋯$F^{\delta-}$); this also results in electrostatic attraction between donor and acceptor (with different directionality characteristics). The typical partial charges involved are roughly 0 to +0.2 e units on H, and depend strongly on the particular system under study [3, 4]. The bond energies of C–H⋯F have been much debated. The energies are small and difficult to determine experimentally [5], so that our knowledge is mainly based on computations. Earlier theoretical studies have been very inconsistent, but modern quantum chemical calculations seem to provide realistic energy estimations, at least for simple molecular systems *in vacuo* (i.e., isolated dimers). Theoretical calculations have shown that the strength of an F⋯H bond could be estimated between 8.0 and 13.4 kJ mol^{-1} [5], lower value corresponding to C–H⋯F hydrogen bond. For comparison, currently, there is consensus that C–H⋯O energies are typically ≤8 kJ mol^{-1} and gradually fade away with increasing H⋯O separation [2, 3]. It must be stressed that the above data are valid only for the particular situation they were calculated for: hydrogen bonds are strongly influenced by their surroundings, such as by the solvent and by other hydrogen bonds, so that interaction strengths in the liquid or solid state will in general case deviate from values mentioned above.

Earlier [5] it has been shown that there are some crystalline structures, where the stability seems to stem from C–F⋯H–C hydrogen bonds. In many cases the distance between fluorine atom and hydrogen atom of second molecule was found to be 2.3 Å, that is, shorter than the sum of the van der Waals radii of the two atoms considered. Moreover, authors [6, 7] studying various F-substituted derivatives of (E)-2,3-diphenyl propenoic acid molecules by experimental (FT-IR spectroscopy) and computational (semiempirical and DTF) methods found that fluorine engaged in C–H⋯F hydrogen bonding easily; the distance of H⋯F is 1.96 to 2.06 Å.

Studying push-pull β-dimethylaminovinyl trifluoromethyl ketone by methods of FTIR, NMR spectroscopy, and quantum chemical calculations we have ascertained that there is additional intramolecular C_β–H⋯F–CF_2 interaction, which stabilizes (EE) conformer. Besides, quantum chemical calculations revealed the distance between hydrogen and fluorine atoms to be quite short (2.409 Å) [8]. Moreover, quantum chemical calculations for various β-dialkylaminovinyl perfluoromethyl ketones also showed a distance H⋯F in (EE) conformers to be in the range 2.379 ÷ 2.436 Å [9]. Continuing to study peculiarities of special and electronic structure of fluor containing enaminoketones we analyzed Fourier IR spectra of (E)-4-(dimethylamino)-1,1,1-trifluorobut-3-en-2-one (DMTBN) and (E)-4-(hexadeutero-dimethylamino)-1,1,1-trifluorobut-3-en-2-one (d_6-DMTBN) enaminoketone in the region of ν(C–H), ν(C=O) and ν(C–F) stretching vibrations. To our knowledge no such study has been carried out until this time, so we have decided to present basic IR experimental data and their interpretation concerning intra-and intermolecular hydrogen bonds of the (DMTBN) and its deuterated analog (d_6-DMTBN).

2. Experimental Section

2.1. General. Carbon tetrachloride was purchased in Aldrich. It was purified using standard techniques and was dried over appropriate drying agent before use.

2.2. Synthesis of Studied Enaminoketone (DMTBN) and Its Deuterated Analog (d_6-DMTBN). The enaminoketone (DMTBN) and its deuterated analog (d_6-DMTBN) have been prepared from thecorresponding alkoxy derivatives [8].

2.3. Infrared Spectra. Infrared spectra were recorded on a Bruker Vertex 70 FTIR spectrometer with KBr beamsplitter and RT-DLaTGS detector at the room temperature (20 ± 1°C). For all spectra 32 scans recorded at 2 cm^{-1} resolution were averaged. Solution spectra were measured in carbon tetrachloride using standard NaCl cells with pathlengths 0.0022, 0.0063 0.01028, 0.0212, 0.0521, and 0.102 cm (for dilution measurements). Temperature measurements were carried out in thermostated (±0.05°C) NaCl cell with pathlength 0.00875 cm. The solutions were scanned at the same conditions as a background. The Bruker Opus software Version 6.0 was used for all data manipulation.

3. Results

IR spectrum of DMTBN is presented on Figure 1. The most intensive bands are in the region of vibrations of double bonds (1700–1500 cm^{-1}) and C–F bonds (1400–1000 cm^{-1}), whereas C–H vibrations are very weak (3100–2800 cm^{-1}).

3.1. The 3100–2700 cm^{-1} Region. In this region the olefinic C–H stretching, symmetric and asymmetric CH_3 stretching bands are expected to be observed. Infrared spectrum of DMTBN shows four weak bands at 3127, 3104, 3059, and 3023 and one very strong and broad band with intricate shape at 2930 cm^{-1}, respectively (Figure 2). Upon deuteration of dimethylamino group four distinct C–H bands are observed at 3134, 3099, 3052, and 3019 cm^{-1} in infrared spectrum of (d_6-DMTBN) (see Figure 3), whereas broad and very intensive band at 2931 cm^{-1} disappears, and two new bands at 2218 and 2072 cm^{-1} appear. As was shown in [10] theoretical calculations predict that the olefinic CH stretching wavenumber should be higher than the wavenumbers of CH_3 stretching

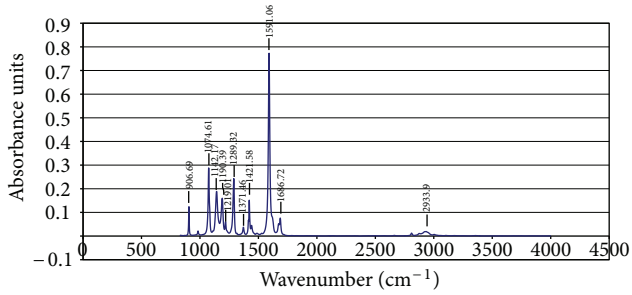

FIGURE 1: IR spectrum of (DMTBN) in CCl_4, $c = 0.03285$ M, $d = 0.01094$ cm.

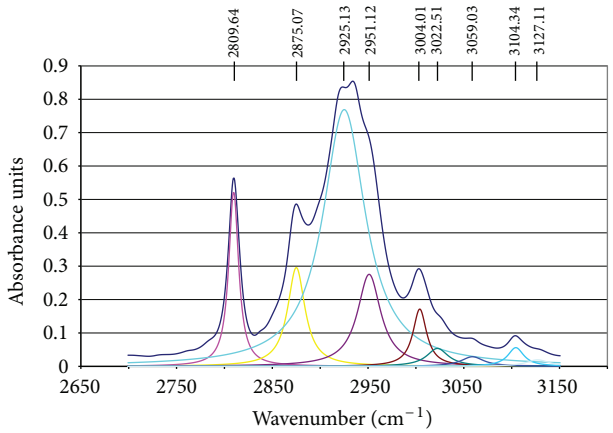

FIGURE 2: Deconvoluted infrared spectrum of DMTBN in CCl_4 in 3150–2700 cm^{-1} region.

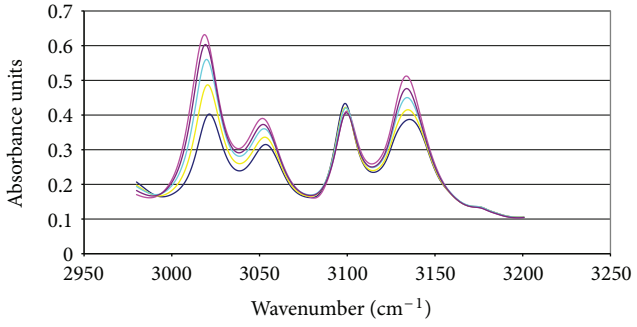

FIGURE 3: Concentration dependence of IR spectrum of d_6-DMTBN in CCl_4.

modes. Therefore, we assigned the bands of d_6-DMTBN at 3134, 3099, 3052, and 3019 cm^{-1} to the olefinic CH stretching modes, whereas the bands at 2218 and 2072 cm^{-1} are attributed to deuterated dimethyl ν(C–D) stretching modes. The main problem is the particular assignment of the olefinic C–H stretching bands. There are two olefinic hydrogen atoms, namely, CH_α and CH_β, in enaminoketones studied. Moreover, as it was shown earlier [8] both DMTBN and d_6-DMTBN are presented in solutions as mixture of (EE) and (EZ) conformers. Hence, it is reasonable to expect four C–H bands, corresponding to CH_α(EE), CH_α(EZ), CH_β(EE), and CH_β(EZ) vibrations. In 1,1,1-trifluoro-2,4-pentanedione [11], which is exclusively in (ZZ) configuration due to intramolecular H-bonding, the olefinic CH_α stretching mode occurs at 3120 cm^{-1}. Similarly, in cis-1,2-difluoroethylene the ν(C–H) wavenumber is 3133 cm^{-1} [4], therefore we ascribed the bands at 3134 and 3099 cm^{-1} to ν(C–H_β) mode. Increase of total concentration of d_6-DMTBN results in increase of intensity of the band at 3134 cm^{-1} with synchronous decrease of intensity of the band at 3099 cm^{-1} (Figure 3).

Temperature rise induces opposite phenomenon: intensity decrease of the former band with simultaneous increase of the latter band. The same effect we have observed earlier for two (C=O) bands of d_6-DMTBN, corresponding to (EE) and (EZ) conformers [8]. In particular, we have showed that concentration increase calls forth intensity increase of (C=O) band of (EE) conformer with simultaneous intensity decrease of (C=O) band of (EZ) conformer, whereas temperature rise has adverse effect. Taking into account this fact we ascribed bands at 3134 and 3099 cm^{-1} to ν(C–H_β) of (EE) and (EZ) conformer, respectively.

After deconvolution of IR spectrum of d_6-DMTBN (see Figure 4) the integrated intensity of each ν(C–H_β) band corresponding to (EE) and (EZ) conformer was calculated according to (1).

$$A = (c_s \times d)^{-1} \times \int_{\text{band}} \log\left(\frac{I_o}{I}\right) d\nu, \tag{1}$$

where A (L mol^{-1} cm^{-2}) is integrated intensity of the ν(C–H_β) band, c_s (mol/L) is the concentration of the given conformer in solution, d (cm) stands for the cell pathlength. The main problem was to evaluate the concentration of each stereoisomeric form c_s. Since all enaminoketones studied were presented as equilibrium (EZ)⇌(EE), which depended on total concentration of enaminoketone and temperature, we used the method, proposed earlier [8] for analysis of conformational equilibria. We plotted integrals of ν(C–H_β) (EZ) versus integrals of appropriate ν(C–H_β) (EE) at various enaminoketone concentrations (c_{total}) provided the product c_{total} × pathlength was constant (Figure 5). Intercepts of this plot with axes were integrals of ν(C–H_β) bands of the (EZ) and (EE) conformer, respectively, but for all that the concentration of the conformer equaled the total concentration of enaminoketone, c_{total}. Knowing the cell pathlength and c_{total}, it was easy to calculate integrated intensities A of the ν(C–H_β) band of each conformer, and, hence, to evaluate from (1) the concentration of each stereoisomeric form, c_s, at given total concentration of enaminoketone. As the consequence it became possible to evaluate the constant K_{eq} of the equilibrium (EZ)⇌(EE). As long as this equilibrium depended on total concentration of enaminoketone [8], we estimated K_{eq} for various concentrations of d_6-DMTBN and plotted ln K_{eq} versus c_{total}. we approximated obtained plot by the (2):

$$\ln K = \ln K_0 + a\left(1 - e^{-bc_{\text{total}}}\right). \tag{2}$$

In Table 1 we listed parameters of (2) calculated for investigated equilibrium from integral intensities of ν(C–H_β).

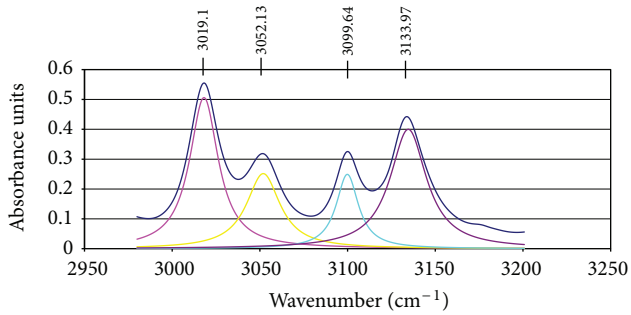

Figure 4: Deconvoluted infrared spectrum of d_6-DMTBN in CCl_4 in 3200–3000 cm^{-1} region.

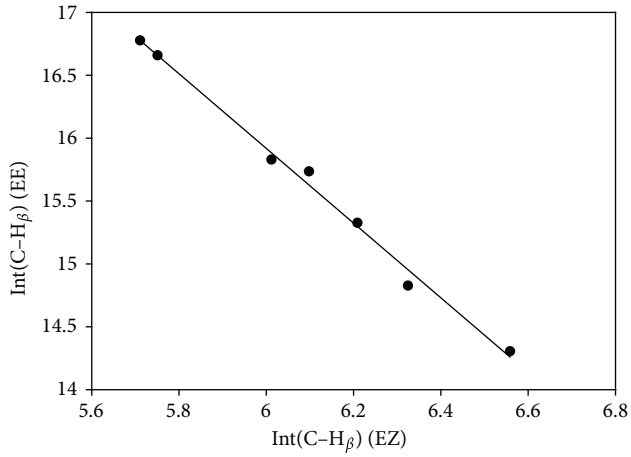

Figure 5: Plot of integral of ν(C–H$_\beta$) of (EE) versus integral of ν(C–H$_\beta$) of (EZ) for d_6-DMTBN in CCl_4.

Second pair of bands, namely, at 3052 and 3019 cm^{-1}, we attributed to ν(C–H$_\alpha$) bands of (EE) and (EZ) conformer, respectively. In contrast to ν(C–H$_\beta$) bands of these conformers an increase of total concentration of d_6-DMTBN resulted in increase of intensity of the both bands (see Figure 3). Using obtained concentrations we calculated integral intensities of ν(C–H$_\alpha$) bands of (EE) and (EZ) conformers, respectively. It turned out that these integral intensities were not constant but depended on total concentration of the enaminoketone (e.g., see Figures 6(a) and 6(b)). Such behavior became clear when we assumed *ad hoc* that (EZ) and (EE) conformers of (d_6-DMTBN) form complexes with intermolecular H$_\alpha$-bonds (Scheme 1). It is well known that complex formation with participation of C–H bond results in increase of intensity [12] and leads to red shift of this band [13, 14], hence integral intensities obtained were the sum of integral intensities of free and bound ν(C–H$_\alpha$).

From (1) it follows that integral of the ν(C–H$_\alpha$) band is expressed by (3):

$$\int_{\text{band}} \log\left(\frac{I_o}{I}\right) d\nu = A_{\text{mon}} \times c_{\text{mon}} + A_{\text{complex}} \times c_{\text{complex}}, \quad (3)$$

Table 1: Parameters of (2) calculated for equilibrium (EZ)⇌(EE) from integral intensities of ν(C–H$_\beta$) and ν(C=O).

Parameter	From intensities of ν(C–H$_\beta$)	From intensities of ν(C=O)
$\ln K_0$	−0.4605	−0.8070
a	0.2428	1.7232
b	17.8790	9.2617
R^2	0.9987	0.9968

where A_{mon} is integral intensity of free ν(C–H$_\alpha$), A_{complex} is integral intensity of bound ν(C–H$_\alpha$), and c_{mon} and c_{complex}—respectively, concentration of free conformer and conformer bound in complex with intermolecular H-bond. Values A_{mon} and A_{complex} for respective conformers were estimated from plots of integral intensities A versus total concentrations of d_6-DMTBN (Figures 6(a) and 6(b). Using (3) together with (4) we calculated concentrations of H-complexes formed by (EE)

$$c_{\text{mon}} + c_{\text{complex}} = c\,(\text{EE, EZ}) \quad (4)$$

and (EZ) conformer and evaluated K_{complex} in assumption that formation of H-complex is in accord with Scheme 1.

As it has turned out a value of K_{complex} for $\nu_{\text{C–H}_\alpha}$(EE) was higher as compared with K_{complex} for $\nu_{\text{C–H}_\alpha}$ (EZ) (cf. 127.04 and 90.57 M^{-1}, resp.).

Increase of total concentration of enaminoketone shifted the bands ν(C–H$_\alpha$) of (EE) and (EZ) conformer to lower wavenumbers (Figures 7(a) and 7(b), whereas wavenumbers of ν(C–H$_\beta$) bands remained almost invariable (the shift does not exceed 1 cm^{-1}). This difference in ν(C–H) behavior is additional vindication of H-complex formation exclusively via C–H$_\alpha$ moiety.

3.2. The 1800–1500 cm^{-1} Region. In IR spectra of (DMTBN) and (DMTBN-d_6) there were two weak ν(C=O) bands at 1686 and 1672 cm^{-1} (DMTBN, in CCl_4) and 1691 and 1671 cm^{-1} (d_6-DMTBN, in CCl_4), respectively. Earlier [8] we ascribed ν(C=O) band with higher wavenumber to the (EZ) and that with lower wavenumber to the (EE) conformer, respectively. The profile of a very intensive ν(C=C) band (Figure 1) *ex facte* creates an impression of single band, but thorough analysis showed [8] that there are two overlapped bands at 1588 and 1593 cm^{-1} (DMTBN), which we attributed to the (EZ) and (EE) conformers, respectively. It is worthy to note that in highly conjugated systems –C=C–C=O ν(C=O) and ν(C=C) vibrations are strongly coupled, possessing, in large measure, the character of out-of-phase and in-phase vibrational modes, respectively [10, 11, 15–17]. Nevertheless, we shall continue to use the ν(C=O) and ν(C=C) as a convenient form of shorthand.

After band fitting the integrated intensity of each ν(C=O) band was calculated according to procedure described for ν(C=O) bands of DMTBN [8]. We calculated K_{eq} for various concentrations of d_6-DMTBN using values $A_{\text{C=O}}$(EZ) and $A_{\text{C=O}}$(EE) (3.36 km M^{-1} and 7.69 km M^{-1}, resp.). Plot of

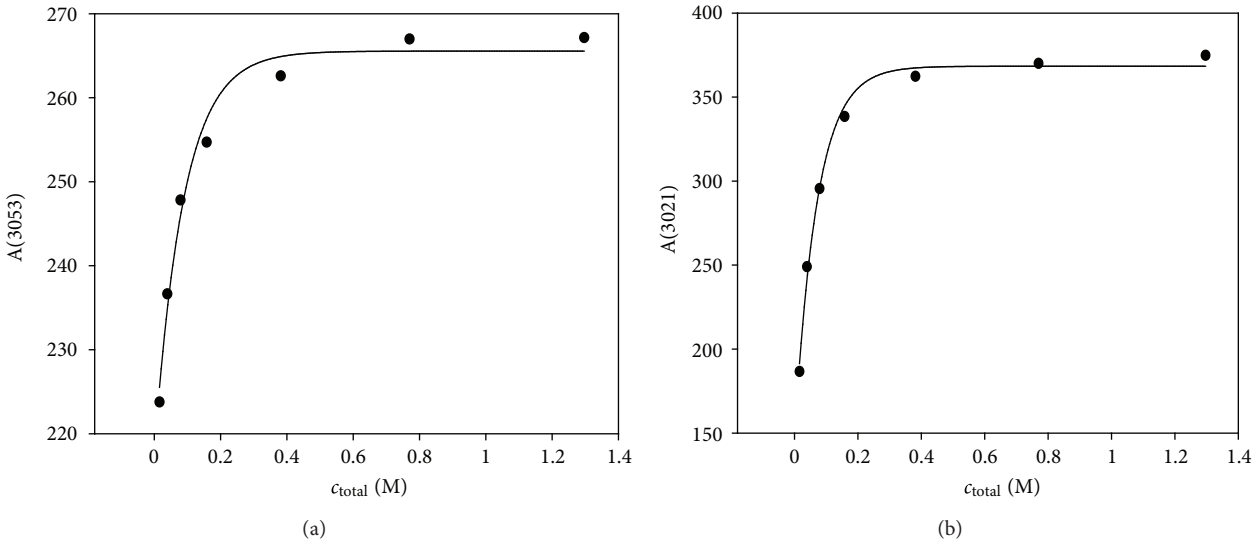

FIGURE 6: Plot of A(C–H_α) versus c_{total} for d_6-DMTBN in CCl_4: (a) for (EE) conformer; (b) for (EZ) conformer.

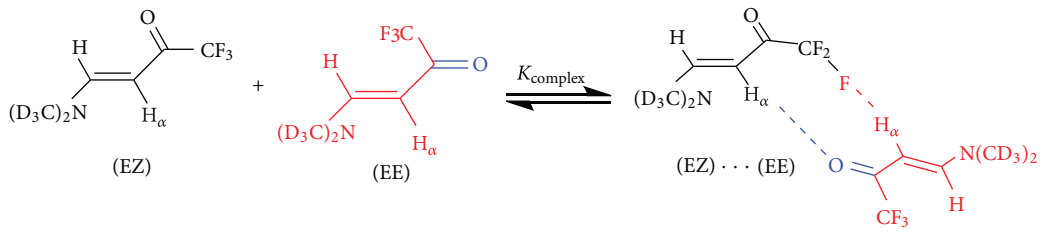

SCHEME 1: Formation of H-bonded "circular" complex between the (EZ) and (EE) conformers.

ln K_{eq} versus c_{total} was exponentially rised described with (2). Parameters of this equation are listed in Table 1.

Temperature measurements of infrared spectrum of d_6-DMTBN gave an opportunity to estimate thermodynamic parameters of equilibrium ΔH_{eq} and ΔS_{eq}, which were equal to 9.86 ± 0.62 kJ M^{-1} and -203.4 ± 2.1 J M^{-1} K^{-1}, respectively. Method of calculation was described in detail elsewhere [8].

It is necessary to note that wavenumbers of $\nu_{C=O}$(EZ) and $\nu_{C=O}$(EE) band behave in different way when total concentration of d_6-DMTBN increases. While the $\nu_{C=O}$(EE) decreases exponentially, the $\nu_{C=O}$(EZ) is virtually stable. Comparing dependence of $\nu_{C=O}$(EE) and $\nu_{C=O}$(EZ) from total d_6-DMTBN concentration one can easily come to conclusion that the carbonyl group of (EE) conformer, in contrast to (EZ) conformer, is incorporated into intermolecular hydrogen bond formation. Therefore, behavior of both $\nu_C - H_\alpha$(EE) (Figure 7) and $\nu_{C=O}$(EE) (Figure 11) indicates C–H_α ⋯O=C bond formation.

3.3. The 1500–800 cm^{-1} Region. In this region of infrared spectrum of (DNTBN) six strong bands at 1421, 1289, 1191, 1142, and 1074 cm^{-1} were observed (Figure 8). Under deuteration the band at 1441 cm^{-1} disappeared, therefore we ascribed it to deformation CH_3 mode. In (trifluoroacetyl) acetone (TAA) this mode was at 1461 and 1413 cm^{-1} [11]. In (TAA), which has the same motif –C=C–C(CF_3)=O the band at 1280 cm^{-1} was attributed to νC–CF_3 + νC = C + δ_sC–CH_3. At the same time authors [11] attributed this band to νC–CH_3 + νC–CF_3 + νCF_3 + νC = C. In 2-thenoyltrifluoroacetone (2-TTA) [18] the bands at 1283, 1279, and 1274 cm^{-1} were assigned to δOH + νC–CF_3 + νC = C + νC-thio + 15. Hence, the band at 1290 cm^{-1} is mainly due to νCF_3 coupled with νC–CF_3 and νC=C. In d_6-DMTBN this band shifted to 1281 cm^{-1} as a result of mass increasing of (CD_3)N–C=C moiety.

Wavenumber and intensity of this band depended on total concentration of d_6-DMTBN and temperature: increase of concentration shifted this band to lower wavenumbers with simultaneous intensity increase (Table 2, Figure 9). As it has been assumed previously (vide supra) CF_3 group participates in intermolecular hydrogen bond C–H⋯F–C (Scheme 1) between (EE) and (EZ) conformer, therefore increase of total concentration of d_6-DMTBN shifted the equilibrium (EZ) + (EE)⇌(EZ)⋯(EE) to the right. Consequently, wavenumber of C–F stretching vibration lowered and the intensity

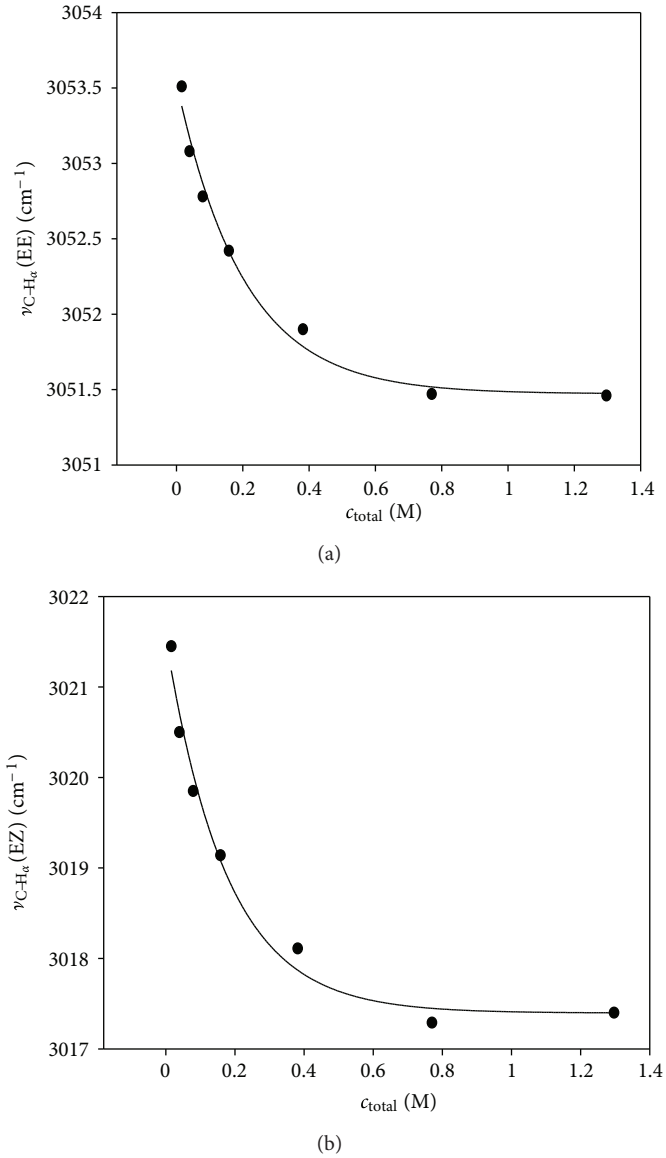

Figure 7: Plot of ν(C–H$_\alpha$) versus c_{total}: (a) for (EE) conformer; (b) for (EZ) conformer.

of this mode increased. Temperature increase shifted the equilibrium to the left, thus increasing wavenumber and decreasing intensity of C–F stretching vibration (Figure 10). The strong band at 1191 cm^{-1} was observed in IR spectrum of DMTBN. Deuteration induced practically no changes on the position of this band: in deuterated d$_6$-DMTBN this band is shifted on 1 cm^{-1} (1190 cm^{-1}, see Figure 9). We assigned this band to ν_aCF3 slightly coupled with δCH$_\alpha$ by analogy with (TAA), where very strong infrared band at 1200 cm^{-1} was correlated to the 1227 cm^{-1} DFT calculated wavenumber, so it was assigned mainly to the CF$_3$ stretching mode coupled to νC–CH$_3$ (12%), δOH (14%), and δCH$_\alpha$ (20%) [10].

In the work [11] this band was assigned to ν_aCF$_3$ + δCH. The band at 1199 cm^{-1} was assigned to ν_αCF$_3$ in 2-TTA [18]. Increase of the concentration of (d$_6$-DMTBN) shifted this band to lower wavenumbers, whereas the intensity was practically invariable (Figure 10). This apparent insensitivity of intensity is a result of cancellation of two effects: increase of CF$_3$ intensity due to participation in intermolecular hydrogen bond C–H⋯F–C and decrease of δCH$_\alpha$ intensity assuming that this deformation vibration refers to δCH$_\alpha$ of the (EZ) conformer, which percentage decreases with concentration increase. Temperature rise shifted this band to higher wavenumbers and decreased its intensity (Table 2). As it clearly can be seen from Figure 10 intensity decrease of this band is much less pronounced than that for band at 1290 cm^{-1} probably due to partial compensation of ν_aCF$_3$ intensity decrease by δCH$_\alpha$(EE) intensity increase.

In spectrum of (DMTBN) there was another strong band at 1142 cm^{-1}, which did not change position under deuteration (Figure 9). We attributed this band to ν_sCF$_3$ coupled to δCH$_\alpha$. In IR spectrum of (TTA) this band is at

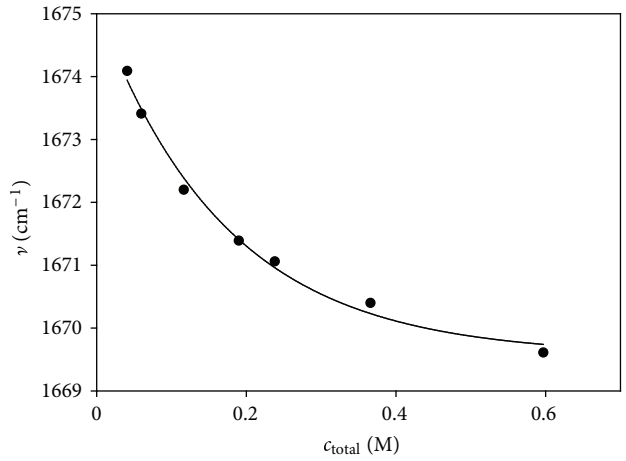

FIGURE 8: Plot of $\nu_{C=O}$(EE) versus c_{total} for d_6-DMTBN in CCl_4.

1180 cm^{-1}. Authors [10] assigned this band to symmetric CF_3 stretching mode, which has been slightly coupled to δCH_α (10%) and δOH (9%). In the work [11] this band was absent, whereas there was a band at 1160 cm^{-1}, which authors assigned to δCH + νC–C + $\nu_s CF_3$. Moreover, in IR spectra of (2-TTA) [18] the bands at 1165 and 1162 cm^{-1} were assigned to $\nu_\alpha CF_3$. Just as the band at 1191 cm^{-1}, concentration rise of (d_6-DMTBN) shifted the band at 1142 cm^{-1} to lower wavenumbers, whereas its intensity changed very slightly (Figure 11). Here again intensity behavior was a consequence of adverse effects: increase of CF_3 intensity due to participation in intermolecular hydrogen bond C–H⋯F–C and decrease of intensity of deformation CH_α vibrations of (EZ) conformer, percentage of which decreased with increase of total (d_6-DMTBN) concentration. Temperature rise shifted this band to higher wavenumbers, simultaneously decreasing its intensity (Table 2). Again, this decrease of intensity was very similar to that of the band at 1191 cm^{-1}, most probably, due to partial compensation of $\nu_\alpha CF_3$ intensity decrease by δCH_α(EZ) intensity increase (see Figure 11).

At last, very strong band at 1074 cm^{-1} (DMTBN, Figure 9), which shifted to higher wavenumbers under deuteration (to 1091 cm^{-1} in IR spectrum of d_6-DMTBN) we attributed to δCH_α, strongly coupled to νCF_3. In IR spectrum of (TAA) this band is observed at 1110 cm^{-1}. Authors [10] assigned it to δCH_α + νCF_3 (31%) + νC–C (15%) mode, whereas in the work [11] the band at 1109 cm^{-1} was assigned to $\nu_s CF_3$ + δCH + νC–C. In (2-TTA) [18] the band at 1110 cm^{-1} was assigned to δCH_α + $\nu_s CF_3$ + νC–C + ν6. In contrast with previously examined bands increase of total concentration of d_6-DMTBN resulted in shift of this band to higher wavenumbers (Table 2) with synchronous increase of its intensity (Figure 10). Bearing in mind the ability of the enaminoketone (d_6-DMTBN) to form complex between (EE) and (EZ) conformers due to intermolecular hydrogen bond C–H⋯F–C (Scheme 1) it is clear that rise of total concentration of (d_6-DMTBN) will increase the percentage of this complex, thus increasing both wavenumber and intensity of δCH_α. On the other hand, temperature rise disrupts the complex, decreasing wavenumber and intensity of deformation C–H_α mode, which prevails in the band at 1047 cm^{-1}.

The band at 906 cm^{-1} shifted to 855 cm^{-1} under deuteration, hence we ascribed it to νN–CH_3 + δC=C–O + νCF_3 + δCH_α by analogy with (TAA) [10, 11].

3.4. Calculation of Thermodynamic Parameters of C–H_α⋯F–C and C–H_α⋯O=C Hydrogen Bonds. Enthalpies of C–H_α⋯F–C and C–H_α⋯O=C bond formation were calculated according to simple (5), derived by Iogansen [12]:

$$-\Delta H = 12.2\,(2)\,\Delta A^{1/2}, \tag{5}$$

where $-\Delta H$ is enthalpy of hydrogen bond formation (kJ dm^3/mol), $\Delta A^{1/2} = A^{1/2} - A_0{}^{1/2}$ denotes the intensity enhancement of the ν(C–H_α) stretching vibration. Values A and A_0 are integral intensity of ν(C–H_α) in monomer and in complex with intermolecular hydrogen bond, respectively. From temperature dependence of profile of ν(C–H_α) bands we calculated K_{complex} (Scheme 1) for various temperatures. Then from plot of $\ln K_{\text{complex}}$ versus $1/T$ (Figure 12) we evaluated enthalpies ($-\Delta H$) and entropies (ΔS) of aforementioned hydrogen bonds. Results obtained are listed in Table 3.

4. Discussion

In Table 4 we listed A_{CH}^{str}, the infrared intensity due to C–H stretching in molecules containing vinyl moiety. According to Equilibrium Charges q and Charge Fluxes ($\partial q_\alpha/\partial R_\tau$) parameterization (ECCF) infrared intensity A_{CH}^{str} can be expressed as in work [4]

$$A_{CH}^{str} \cong \left|\frac{\partial \mu_{CH}}{\partial r_{CH}}\right|^2 = \left|q_H^0 + \frac{\partial q_H}{\partial r_{CH} \times r_{CH}^o}\right|, \tag{6}$$

where $\partial\mu_{CH}/\partial r_{CH}$ and $\partial q_H/\partial r_{CH}$ are, respectively, the derivative of the electrical dipole moment μ of C–H bond and charge q_H referred to hydrogen atom with respect of the interatomic distance r_{CH}, and q_H^0 is an equilibrium charge referred to hydrogen atom. Gussoni et al. [19–22] found that q_H^0 and $\partial q_H/\partial r_{CH}$ are very important markers of the charge distribution inside the molecule and are directly related to the molecule structure, the vibration potential, and the molecular conformation. In particular, from (6) it follows that when the charge flux is sizable, both q_H^0 and $\partial q_H/\partial r_{CH}$ give a considerable contribution to A_{CH}^{str}. When the carbon atom has either sp^2 or sp^3 hybridization the flux $\partial q_H/\partial r_{CH}$ is practically constant and amounts approximately to −0.2 e/Å [22]. Since the equilibrium charge on hydrogen is always positive in C–H bonds and turns out to be always less than 0.2 e, when carbon atom has sp^2 or sp^3 hybridization, $\partial q_H/\partial r_{CH}$ is negative, but its absolute value decreases when the charge increases and so does the A_{CH}^{str}. This effect is clearly observed passing from ethane to 1.1-difluoroethylene and 1.2-difluoroethylene (Table 4). Increase of ν_{CH}^{str} with

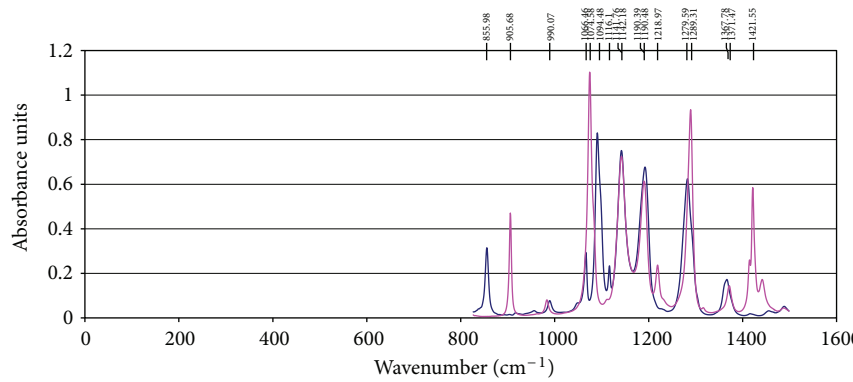

Figure 9: Spectrum of enaminoketone DMTBN (thick line) and d_6-DMTBN (thin line) in the region of C–F vibrations.

Table 2: Dependence of wavenumbers and intensities of CF_3 stretching vibrations on concentration of d_6-DTNBN and temperature.

Wavenumber		Intensity	
Concentration increase	Temperature increase	Concentration increase	Temperature increase
Band at 1280 cm^{-1} ($\nu CF_3 + \nu C{-}CF_3 + \nu C{=}C$)			
Decreases	Increases	Increases	Decreases
Band at 1190 cm^{-1} ($\nu_a CF_3 + \delta CH_\alpha$)			
Decreases	Increases	Very weak dependence	Decreases
Band at 1142 cm^{-1} ($\nu_s CF_3 + \delta CH_\alpha$)			
Decreases	Increases	Very weak dependence	Decreases
Band at 1090 cm^{-1} ($\delta CH_\alpha + \nu_s CF_3$)			
Increases	Decreases	Increases	Decreases

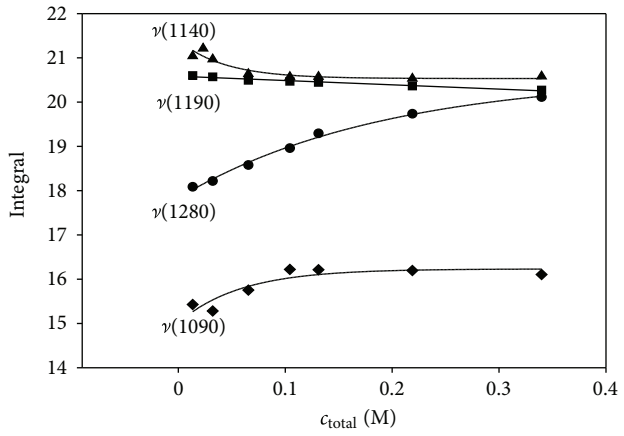

Figure 10: Plots of integral versus c_{total} for bands at 1280, 1190, 1142, and 1190 cm^{-1} of d_6-DMTBN (in CCl_4).

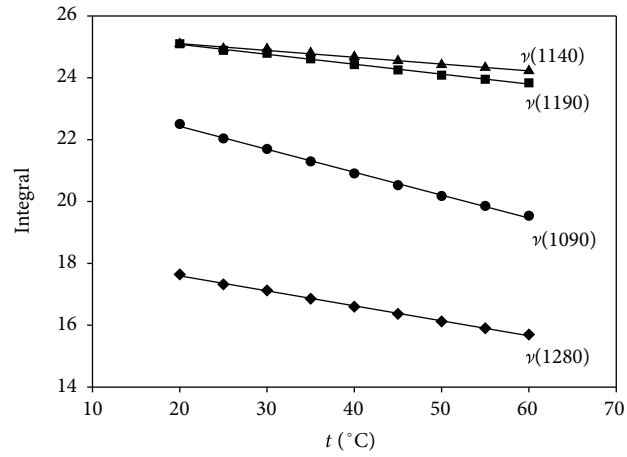

Figure 11: Plots of integral versus t°C for bands at 1280, 1190, 1142, and 1190 cm^{-1} of d_6-DMTBN (in CCl_4).

simultaneous decrease of A^{str}_{CH} indicates that introduction of fluorine to an ethylene molecule induces a stronger polarization of a CH bond, which makes the q^0_H charge to increase; also force constant (k_{CH}) increases while r^0_{CH} and A^{str}_{CH} decrease [4]. Backdonation also may take place, but its role in fluorinated ethylenes is insignificant. Induction of stronger polarization of CH bond occurs when an electronegative atom is in molecule: influence of nitrogen in the studied enaminoketones invokes the same effect on adjacent C_β–H bond as a fluorine atom in substituted ethylenes (Table 4). As is obvious from Table 4 wavenumber ν^{str}_{CH} of C_β–H bond for (EE) conformer is significantly higher then for (EZ) conformer of (d_6-DMTBN). Decrease of wavenumber ν^{str}_{CH} in the (EZ) conformer as compared to it in the (EE) conformer is a result of stronger polarization of C_α–H bond in former one which makes the q^0_H charge increase, as a consequence k_{CH} also increases. It should be expected that A^{str}_{CH} decreases when equilibrium charge q^0_H increases but integral intensity

Table 3: Thermodynamic parameters of =C–H_α ⋯F–C and =C–H_α ⋯O=C hydrogen bonds.

Method	=C–H_α ⋯F–C hydrogen bond		=C–H_α ⋯O=C hydrogen bond	
	$-\Delta H$ kJ mol^{-1} dm^3	ΔS J mol^{-1} dm^3 K^{-1}	$-\Delta H$ kJ mol^{-1} dm^3	ΔS J mol^{-1} dm^3 K^{-1}
From (5)	6.09[a]	—	27.48[b]	—
From (5)[b]	—	—	24.19[c]	—
From temperature measurement	6.71 ± 0.10	−213.3 ± 0.4	21.70 ± 0.66	−156.3 ± 2.3

[a] Using $A_{C\text{–}H_\alpha}(EE)_{mon}$ = 21.77 cm mmol^{-1}, $A_{C\text{–}H_\alpha}(EE)_{H\text{-complex}}$ = 26.70 cm mmol^{-1}.
[b] Using $A_{C\text{–}H_\alpha}(EZ)_{mon}$ = 14.71 cm mmol^{-1}, $A_{C\text{–}H_\alpha}(EZ)_{H\text{-complex}}$ = 37.00 cm mmol^{-1}.
[c] Using $A_{C=O}(EE)_{mon}$ = 1204.28 cm mmol^{-1}, $A_{C=O}(EE)_{H\text{-complex}}$ = 1345.44 cm mmol^{-1}.

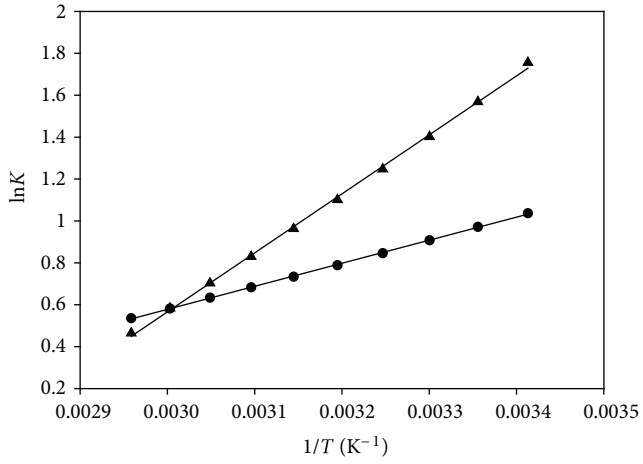

Figure 12: Plot of ln $K_{H\cdots F}$ and ln $K_{H\cdots O}$ versus $1/T$ for d_6-DMTBN in CCL_4. ln $K_{H\cdots F} = -2.72343 + 1100.44 * 1/T$. ln $K_{H\cdots O} = -7.882 + 2816.2 * 1/T$.

A^{str}_{CH} of the (EE) conformer is considerably larger than A^{str}_{CH} of the (EZ) conformer. As was stated earlier [8] H_β hydrogen atom is involved in formation of intramolecular C_β–H⋯F–C hydrogen bond, hence A^{str}_{CH} is increased in the (EE) conformer as a result of increase of the effective charge $\partial\mu/\partial r$ in (7), which characterizes the additive model of H-bond [12]:

$$\left(\frac{\partial\mu}{\partial r}\right) = \left(\frac{\partial\mu_0}{\partial r}\right) + \left(\frac{\partial\mu_H}{\partial r_H}\right), \quad (7)$$

where $\partial\mu_0/\partial r$ and $\partial\mu_H/\partial r_H$ are effective charges of C–H and H⋯F bonds, respectively.

Wavenumbers ν^{str}_{CH} of C_α–H stretching vibration of the (EE) and (EZ) conformers are lower than that of C_β–H mode although electron withdrawal power of trifluorocarbonyl group is much higher comparing with dimethylamino group. It is obvious that in highly conjugated systems similar to enaminoketones [8, 9] complicated variations in the charge fluxes take place, and any analysis based only on variations of the charge may turn out to be incorrect, therefore we believe that much more ECCF investigations of various conjugated molecules should be obtained before deriving any conclusion. It is notable that difference in $A^{str}_{C_\alpha H}$ values of the (EE) and (EZ) conformer is small (0.6 km mol^{-1} dm^3) and significantly lower than difference in $A^{str}_{C_\beta H}$ of respective conformers (2.8 km mol^{-1} dm^3). We attributed this fact to

Table 4: Wavenumbers $\nu^{str}_{C\text{–}H}$ and integral intensities $A^{str}_{C\text{–}H}$ of C–H bonds of vinyl moiety. To avoid ambiguities italics indicates the CH_x group to which refers. In parentheses relevant isomer/conformer is denoted.

	$\nu^{str}_{C\text{–}H}$ (cm^{-1})	$A^{str}_{C\text{–}H}$ (km mol^{-1} dm^3)
C_2H_4	3055 [4]	9.6[a] [4]
CHF=C*H*F	3122 (Z) [4]	3.7[a] [4]
CHF=C*H*F	— (E) [4]	4.75[a] [4]
CF_2=CH_2	3133 [4]	2.1 [4]
$(CD_3)_2$N–CH=C*H*(CF_3)=O	3135 (EE)	4.27
	3099 (EZ)	1.44
$(CD_3)_2$N–CH=C*H*(CF_3)=O	3053 (EE)	2.18
	3051 (EE)[b]	2.67[b]
	3021 (EZ)	1.47
	3017 (EZ)[c]	3.70[c]
$(CH_3)_2$N–C*H*=CH(CF_3)=O	3124 (EE)	—
	3104 (EZ)	—
$(CH_3)_2$N–CH=C*H*(CF_3)=O	3058 (EE)	—
	3023 (EZ)	—

[a] A^{str}_{CH}(av) is the average IR intensity per CH (i.e., the infrared intensity of the stretching region divided by the number of CH bonds).
[b] Wavenumber $\nu^{str}_{C\text{–}H}$ and integral intensity $A^{str}_{C\text{–}H}$ of C–H_α bond involved in C–H⋯F hydrogen bond.
[c] Wavenumber $\nu^{str}_{C\text{–}H}$ and integral intensity $A^{str}_{C\text{–}H}$ of C–H_α bond involved in C–H⋯O=C hydrogen bond.

Table 5: Assignment of some fundamental bands in IR spectrum of d_6-DMTBN (in CCl_4).

Wavenumber, cm^{-1}	Assignment
3134	νCH_β(EE)
3099	νCH_β(EZ)
3042	νCH_α(EE)
3019	νCH_α(EZ)
1691	ν_aO=C–C=C(EZ)
1671	ν_aO=C–C=C(EE)
1281	$\nu CF_3 + \nu$C–$CF_3 + \nu$C=C
1190	$\nu_a CF_3 + \delta CH_\alpha$
1142	$\nu_s CF_3 + \delta CH_\alpha$
1091	δCH + $\nu_s CF_3$
855	νN–$CD_3 + \delta$C=C + $\nu CF_3 + \delta CH_\alpha$

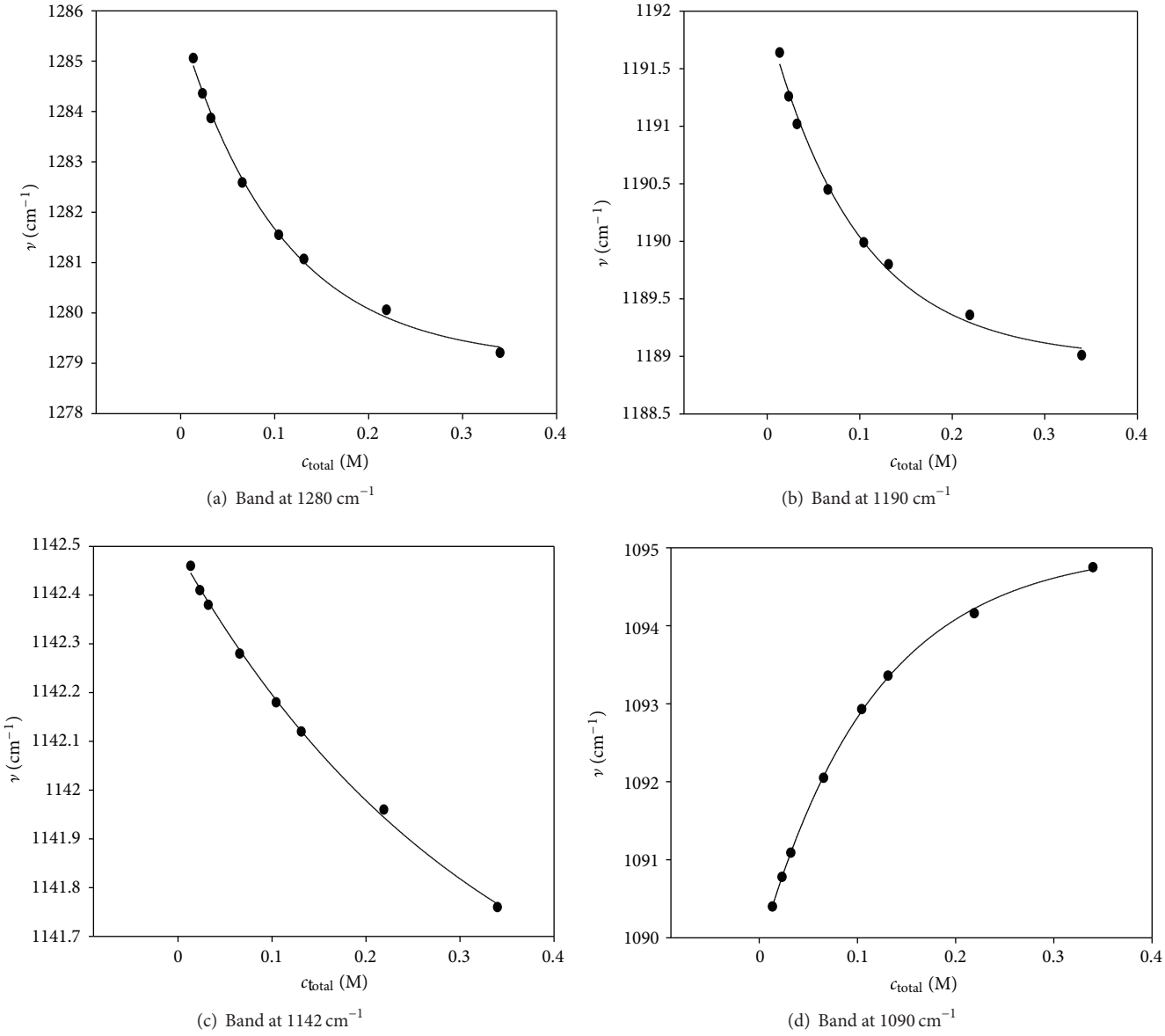

(a) Band at 1280 cm^{-1}

(b) Band at 1190 cm^{-1}

(c) Band at 1142 cm^{-1}

(d) Band at 1090 cm^{-1}

Figure 13: Plots of ν (C–F)[a] versus concentration of d_6-DNTBN. [a]Band attribution is given in Table 5.

the involvement of C_β–H bond in intramolecular C_β–H⋯F hydrogen bond.

Concentration dependence of profile of IR spectrum of (d_6-DMTBN) in the region of ν^{str}_{CH} vibrations reflects not only conformation equilibrium (EZ)⇌(EE), but also equilibrium between monomeric conformers and their H-bonded complex (see Scheme 1). Moreover, analysis of profile of IR spectra of (DMTBN) and (d_6-DMTBN) in the region of carbonyl vibrations revealed that the only $\nu^{str}_{C=O}$ of (EE) conformer shifts to lower wavenumbers with increase of enaminoketone concentration (see Figure 8), whereas $\nu^{str}_{C=O}$ of the (EZ) conformer is independent of enaminoketone C_{total}. Therefore, we reached a conclusion that carbonyl of the (EE) conformer takes part in formation of intermolecular H-bond with C–H_α of the (EZ) conformer. Simultaneously intermolecular C–H_α⋯F–C bond is formed, thus cyclic dimer appears as it is presented on Scheme 1. Considering that H-complex is 1 : 1 we evaluated equilibrium constant $K_{H\text{-complex}}$ for both C–H_α⋯O=C and C–H_α⋯F–C hydrogen bond from (8):

$$K_{H\text{-complex}} = \frac{C_{H\text{-complex}}}{C(EE)_{mon} \times C(EZ)_{mon}}. \quad (8)$$

Equilibrium constant $K_{H\text{-complex}}$ for C–H_α⋯O=C H-bond formation is much higher than that for C–H_α⋯F–C bond formation (viz., 214.4 and 16.4 M^{-1}). Enthalpy of hydrogen bond formation (ΔH), evaluated from temperature dependence of $K_{H\text{-complex}}$, revealed that ΔH for C–H_α⋯O=C H-bond is more negative than that for C–H_α⋯F–C, hence the former H-bond is stronger as compared with the latter (cf. values of −21.7 and −6.7 kJ mol^{-1} dm^3, resp., Table 3).

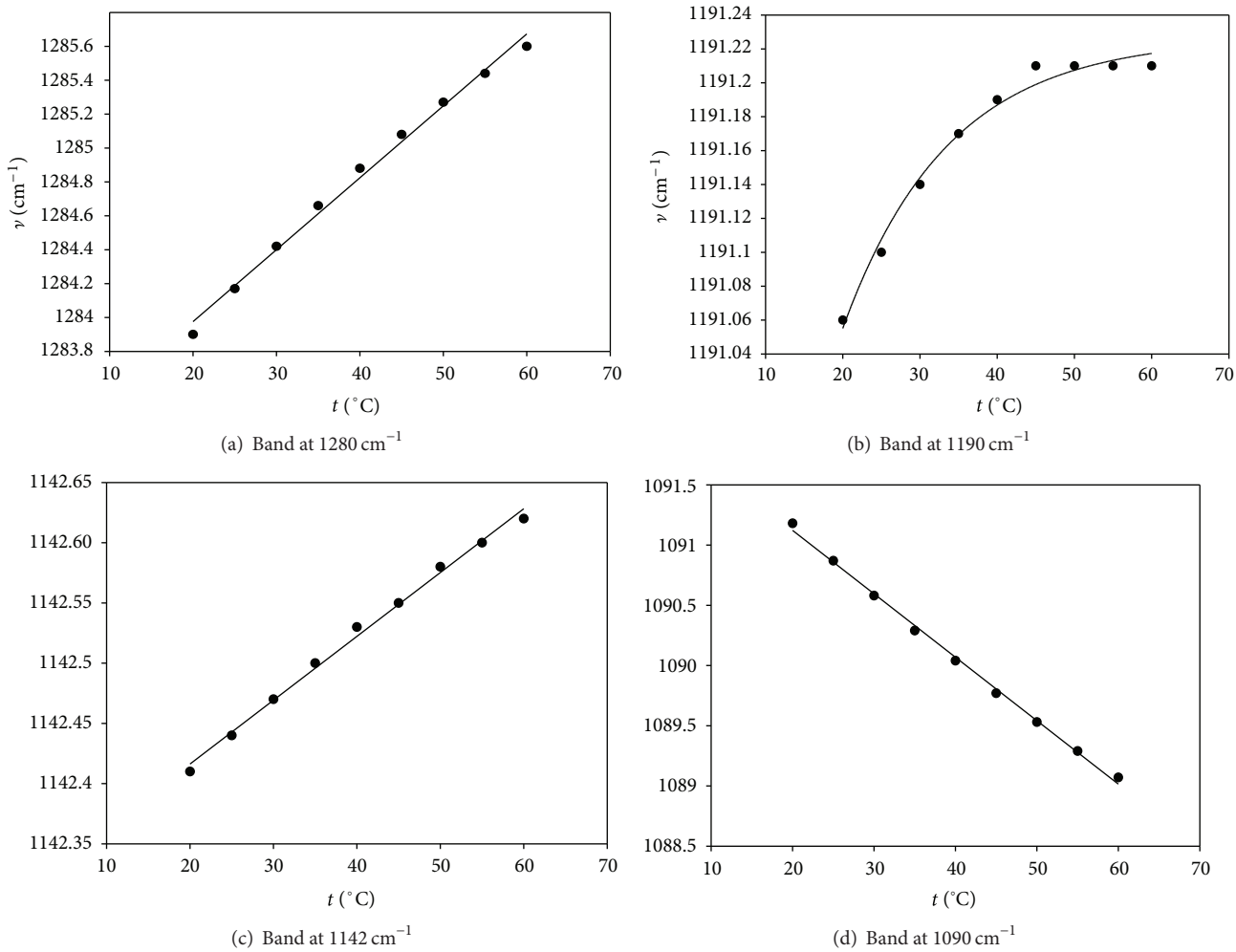

(a) Band at 1280 cm^{-1}

(b) Band at 1190 cm^{-1}

(c) Band at 1142 cm^{-1}

(d) Band at 1090 cm^{-1}

FIGURE 14: Plots of ν(C–F)[a] versus t°C for d_6-DNTBN in CCl_4. [a]Band attribution is given in Table 5.

Thus, when concentration of (d_6-DMTBN) increases, dimer between the (EE) and (EZ) conformers is formed due to intermolecular H-bonds, more strong H-bond C–H_α ⋯O=C forms in the first place, whereas the bond C–H_α ⋯F–C forms afterward. It is notable that enthalpies of H-bond formation, evaluated from Iogansen equation (5) and from temperature measurements, are in good agreement (see Table 3). Nevertheless, some discrepancies arise from insufficient accuracy in evaluation of A_{mon}.

As it was established earlier [8] there is an intramolecular H-bond C–H_β ⋯F–C in the (EE) conformer of (d_6-DMTBN), therefore thermodynamic parameters evaluated for equilibrium (EZ)⇌(EE) are complex and combine parameters of an intramolecular C–H_β ⋯ F–C and intermolecular H-bonds (see Scheme 1) in accord with (9). In other words, conversion of the (EE) conformer to the (EZ) conformer, which takes place during dilution of (d_6-DMTBN) solution or at temperature rise, is accompanied with breaking of the intra- and intermolecular hydrogen bonds:

$$\Delta H_{\text{total}} = \Delta H_{\text{conf}} + \Delta H_{\text{intra}} + \Delta H_{\text{inter}}, \quad (9)$$

where ΔH_{total}, ΔH_{conf}, ΔH_{intra}, and ΔH_{inter} are enthalpy of equilibrium (EZ)⇌(EE) evaluated experimentally from temperature measurements (Table 3), true enthalpy of this equilibrium, enthalpy of an intramolecular H-bond C–H_β ⋯F–C formation, and enthalpy of an intermolecular C–H_α ⋯F–C and C–H_α ⋯O=C H-bond formation, respectively.

Using (9) and assuming value ΔH_{intra}, to be close to that of an intermolecular C–H_α ⋯F–C H-bond formation (ca −6.7 kJ mol^{-1} dm^3) we calculated ΔH_{conf} which turned out to be positive and equaled 25.3 kJ mol^{-1} dm^3. This value consists of enthalpy of equilibrium (EZ)⇌(EE) evaluated experimentally for $(CD_3)_2$N–CH=CH–C(O)CH_3 (with respect to 16.4 kJ mol^{-1} dm^3 [8]) where formation of intramolecular H-bond and cyclic dimer is impossible. Moreover, DFT calculations revealed that the (EZ) conformer of (DMTBN) is more stable than the (EE) conformer [8]. This result conforms to positive enthalpy of equilibrium (EZ)⇌(EE) (see above), thus confirming validity of supposition of intra- and intermolecular H-bond formation in studied enaminoketones.

Intermolecular C–H_α ⋯F–C hydrogen bond formation has considerable impact on C–F vibrations at 1280 ÷ 1090 cm^{-1}. So far as these vibrations were coupled with

deformation δCH_α vibrations (see Table 5), the influence of C–H_α ⋯F–C hydrogen bond was ambiguous. The band νCF_3 at 1281 $cm^{-1}$was not coupled with δCH_α, therefore increase of (d_6-DNTBN) concentration changed both wavenumber and intensity of this vibration. It is well known that participation in hydrogen bonding, even relatively weak, shifts the band to lower wavenumbers with synchronous intensity increase [12]. As can be seen from Figure 13(a) this increase shifted the band at 1281 cm^{-1} to lower wavenumbers significantly with appreciable intensity increase (Figure 10). On the other hand, vibrations $\nu_a CF_3$ and $\nu_s CF_3$ (at 1190 and 1142 cm^{-1}, resp.), strongly coupled with δCH_α, shifted to lower wavenumbers in much lesser degree (in comparison with bond at 1281 cm^{-1}) when concentration of (d_6-DNTBN) increased. Intensities of these bands also decreased insignificantly (Figure 10). In this case we observed the result of cancellation of two effects: increasing of concentration of complex with C–H_α ⋯F–C bond and simultaneous decrease of the (EZ) conformer concentration. Contribution of δCH_α(EZ) decreased, thus compensating the increase of intensity of ν(C–F) vibration. Temperature rise disrupted C–H_α ⋯F–C bond but simultaneously increased concentration of (EZ) conformer, therefore decrease of wavenumbers and intensities of these bands is negligible (see Figures 14 and 11, resp.). At the same time the band $\nu(CF_3)$ at 1091 cm^{-1} was strongly coupled with δCH. Moreover, contribution of the latter mode exceeded the contribution of the former vibration, therefore behavior of this band differed from behavior of other bands examined above. Increase of (d_6-DNTBN) concentration shifted this band to higher wavenumbers (Figure 13(d)) with simultaneous increase of band intensity (Figure 10). The observed effect was a result of involvement of C–H into intermolecular C–H⋯F–C H-bonding [23] in cyclic dimer, which concentration rised when total concentration of enaminoketone increased. Temperature increase broke this hydrogen bond, thus shifting δCH to lower wavenumbers and diminishing band intensity.

5. Conclusion

There are four bands in IR spectra of studied enaminoketone (DNTBN) and its deuterated analog (d_6-DNTBN) in the region of ν(C–H), corresponding to $\nu^{EE}_{CH_\alpha}$, $\nu^{EZ}_{CH_\alpha}$, $\nu^{EE}_{CH_\beta}$, and $\nu^{EZ}_{CH_\beta}$; ν_{CH} of the (EE) conformer being at higher wavenumbers than ν_{CH} of the (EZ) conformer. Wavenumbers and intensities of these bands depend not only on temperature, but also on concentration of enaminoketone, thus reflecting presence of two kinds of equilibrium: equilibrium of the (EE) and (EZ) conformer, and equilibrium between monomeric conformers and their dimer. While variations of wavenumbers and intensities of $\nu^{EE}_{CH_\beta}$ and $\nu^{EZ}_{CH_\beta}$ vibrations are called forth by changes in the conformer equilibrium exclusively, appropriate variations of wavenumbers and intensities of $\nu^{EE}_{CH_\alpha}$ and $\nu^{EZ}_{CH_\alpha}$ vibrations are caused by changes of both conformer and monomer-dimer equilibrium. Increase of enaminoketone concentration shifts the equilibrium (EZ)⇌(EE) to the right, thus increasing equilibrium constant, K_{eq}. Simultaneously the equilibrium (EZ) + (EE)⇌(EZ⋯EE) is shifted towards cyclic dimer, which formation is due to intermolecular C–H_α ⋯O=C and C–H_α ⋯F–C hydrogen bonds. Evaluation of constant $K_{H\text{-complex}}$ and enthalpy of formation of these H-bonds (ΔH) revealed that C–H_α ⋯O=C bond has greater $K_{H\text{-complex}}$ and more negative ΔH than the C–H_α ⋯F–C H-bond. As a consequence, the former bond is formed at first, whereas the latter bond being weaker is generated much slower. Evaluation of true enthalpy of the equilibrium (EZ)⇌(EE) revealed that the value of ΔH is positive, thus conforming with results of DFT calculations, according to which the (EZ) conformer is more stable than the (EE) one. Formation of the C–H_α ⋯F–C hydrogen bond effects ν^{str}_{CF} vibrations, but analyzing this influence one must take into account that these vibrations in some cases are coupled with δ_{CH_α}.

References

[1] A. Allerhand and P. V. R. Schleyer, "A survey of C–H groups as proton donors in hydrogen bonding," *Journal of the American Chemical Society*, vol. 85, no. 12, pp. 1715–1723, 1963.

[2] G. A. Jeffrey and W. Saenger, *Hydrogen Bonding in Biological Structures*, Springer, Berlin, Germany, 1991.

[3] T. Steiner, "Unrolling the hydrogen bond properties of $C - H \cdots O$ interactions," *Chemical Communications*, pp. 727–734, 1997.

[4] M. Gussoni and C. Castiglioni, "Infrared intensities. Use of the CH-stretching band intensity as a tool for evaluating the acidity of hydrogen atoms in hydrocarbons," *Journal of Molecular Structure*, vol. 521, no. 1–3, pp. 1–18, 2000.

[5] J. P. Bégué and D. Bonnet-Delton, "Biological impacts of fluorination: pharmaceuticals based on natural products," in *Fluorine and Health. Molecular Imaging, Biomedical Materials and Pharmaceuticals*, A. Tressaud and G. Haufe, Eds., p. 554, Elsevier, Amsterdam, The Netherlands, 2008.

[6] J. T. Kiss, K. Felföldi, and I. Pálinko, "Changes in the aggregation patterns of *Z*-2,3-diphenylpropenoic acid and its methyl ester on substituting the olefinic hydrogen with CF_3 group-an FT-IR study," *Journal of Molecular Structure*, vol. 744–747, pp. 207–210, 2005.

[7] B. Tolnai, J. T. Kiss, K. Felföldi, and I. Pálinko, "C– H⋯F hydrogen bonds as the organising force in F-substituted α-phenyl cinnamic acid aggregates studied by the combination of FTIR spectroscopy and computations ," *Journal of Molecular Structure*, vol. 924–926, p. 27, 2009.

[8] S. I. Vdovenko, I. I. Gerus, and V. P. Kukhar, "Conformational analysis of push-pull enaminoketones using Fourier transform IR, NMR spectroscopy, and quantum chemical calculations. I. β-Dimethylaminovinyl methyl ketone, β-dimethylaminovinyl trifluoromethyl ketone and their deuterated derivatives," *Vibrational Spectroscopy*, vol. 52, pp. 144–153, 2010.

[9] S. I. Vdovenko, I. I. Gerus, V. Olga Balabon, and V. P. Kukhar, "The conformational analysis of push- pull enaminoketones using Fourier transform IR and NMR spectroscopy, and quantum chemical calculations. III. alfa-Dialkylaminovinyl perfluoromethyl ketones and alfa-dialkylaminovinyl trichloromethyl ketones," *Trends in Organic Chemistry*. In press.

[10] H. Raissi, A. Nowroozi, M. Roozbeh, and F. Farzad, "Molecular structure and vibrational assignment of (trifluoroacetyl) acetone: a density functional study," *Journal of Molecular Structure*, vol. 787, no. 1–3, pp. 148–162, 2006.

[11] M. Zahedi-Tabrizi, F. Tayyari, Z. Moosavi-Tekyeh, A. Jalali, and S. F. Tayyari, "Structure and vibrational assignment of the enol form of 1,1,1-trifluoro-2,4-pentanedione," *Spectrochimica Acta A*, vol. 65, no. 2, pp. 387–396, 2006.

[12] A. V. Iogansen, "Direct proportionality of the hydrogen bonding energy and the intensification of the stretching ν (XH) vibration in infrared spectra," *Spectrochimica Acta A*, vol. 55, no. 7-8, pp. 1585–1612, 1999.

[13] P. J. A. Ribeiro-Carlo and P. D. Vaz, "Towards the understanding of the spectroscopic behaviour of the C–H oscillator in $C - H \cdots O$ hydrogen bonds: the effect of solvent polarity," *Chemical Physics Letters*, vol. 390, pp. 358–361, 2004.

[14] G. Lui, L. Ping, and H. Li. Spectrochim, "$C - H \cdots O$ hydrogen bond in chloroform-triformylmethane complex: blue-shifted or red-shifted?" *Acta Part A*, vol. 66, pp. 643–645, 2007.

[15] P. J. Taylor, "The i.r. spectroscopy of some highly conjugated systems-I. Rationale of the investigation," *Spectrochimica Acta A*, vol. 32, no. 8, pp. 1471–1476, 1976.

[16] R. A. Nyquist, *Interpreting Infrared, Raman, Nuclear Magnetic Resonance Spectra*, vol. 1, Academic Press, 2001.

[17] D. Smith and P. J. Taylor, "The i.r. spectroscopy of some highly conjugated systems-II. Conformational effects in simple enamino-ketones. A note on 4-pyridone," *Spectrochimica Acta A*, vol. 32, no. 8, pp. 1477–1488, 1976.

[18] A. R. Nekoe, S. F. Tayyari, M. Vakii, S. Holakoei, A. H. Hamodian, and R. E. Sammelson, "Conformation and vibrational spectra and assignment of 2-thenoyltrifluoroacetone," *Journal of Molecular Structure*, vol. 932, pp. 112–122, 2009.

[19] M. Gussoni, "Role of vibrational intensities in the determination of molecular structure and charge distribution," *Journal of Molecular Structure*, vol. 113, pp. 323–340, 1984.

[20] M. Gussoni, C. Casiglioni, and G. Zerbi, "Physical meaning of electrooptical parameters derived from infrared intensities," *Journal of Physical Chemistry*, vol. 88, p. 341, 1984.

[21] M. Gussoni, "Infrared intensities: a new tool in chemistry," *Journal of Molecular Structure*, vol. 141, pp. 63–92, 1986.

[22] C. Casiglioni, M. Gussoni, and G. Zerbi, "Characteristic infrared intensities of CH bonds," *Journal of Molecular Structure*, vol. 141, pp. 341–346, 1986.

[23] A. V. Iogansen, "IK-spektroskopiya i opredeleniye energii vodorodnoy svyazi (IR-spectroscopy and evaluation of hydrogen bond energy)," in *Vodorodnaya Svyaz (the Hydrogen Bond)*, N. D. Sokolov, Ed., pp. 112–155, Izd. Nauka, Moscow, Russia, 1981.